J. Fluid Mech. (1985), *vol.* 153, *pp.* 479–499
Printed in Great Britain

When and where to put a discharge in an oscillatory flow

By RONALD SMITH

Department of Applied Mathematics and Theoretical Physics, University of Cambridge, Silver St, Cambridge CB3 9EW

(Received 31 January 1984 and in revised form 22 November 1984)

Exact results are derived for the centroid and longitudinal variance of a passive contaminant distribution at large times after an instantaneous discharge in an oscillatory flow in a straight channel of constant cross-section. It is shown that the precise timing and cross-stream position of the discharge can have a substantial and persistent influence.

1. Introduction

For steady flows in rivers Smith (1981, 1984) and Daish (1985) have shown that the cross-stream location of an instantaneous contaminant release can have a persistent and marked effect upon the concentrations experienced far downstream; while, for uniform discharges in oscillatory flows, Allen (1982, figure 8) and Smith (1982, figures 2*a–c*) have drawn attention to the importance of the timing of the contaminant release. The purpose of the present paper is to encompass both these features and to investigate the long-term influence of the precise timing and cross-stream position of a discharge in an oscillatory flow.

The first few sections of this paper are directed towards the derivation of an exact expression for the longitudinal variance of a passive contaminant at large times after discharge in an oscillatory flow in a straight channel of constant cross-section. This exact result is then used to illuminate several facets of the dispersion process. First, an analytic expression is derived for an alternative definition of the shear dispersion coefficient proposed by Yasuda (1982). It is confirmed that, unlike the conventional definition, the new definition does not suffer from the anomaly of having negative values (Chatwin 1975). Secondly, results derived by Smith (1983, equation (6.6)) for a particular flow, concerning the optimal timing of uniform discharges, are shown to have general validity. Thirdly, the title problem is addressed, and it is considered when and where to put a discharge in an oscillatory flow so that the spread of contaminant at large times is maximized (i.e. the concentration is minimized). Finally, the general principles are illustrated using a simple mathematical model for contaminant dispersion in a vertically well-mixed estuary of parabolic cross-section.

2. Moment equations

In axes moving with the bulk velocity $\bar{u}$, the concentration $c(x, y, z, t)$ of a passive contaminant in a longitudinally uniform plane parallel flow satisfies the advection–diffusion equation

$$\partial_t c + (u-\bar{u})\,\partial_x c - \kappa_{11}\,\partial_x^2 c - \boldsymbol{\nabla}\cdot(\boldsymbol{\kappa}\cdot\boldsymbol{\nabla} c) = q(y,z)\,\delta(t-t_0)\,\delta(x-x_0), \tag{2.1a}$$

with

$$\boldsymbol{n}\cdot\boldsymbol{\kappa}\cdot\boldsymbol{\nabla} c = 0 \quad \text{on } \partial A. \tag{2.1b}$$

Here $u(y,z,t)$ is the longitudinal velocity, $\kappa_{11}(y,z,t)$ the longitudinal diffusivity, $\boldsymbol{\varkappa}$ the transverse diffusivity tensor, ∇ the transverse gradient operator, t_0 the time of release, x_0 the release position, $q(y,z)$ the discharge shape, ∂A the impermeable boundary and $\boldsymbol{n}$ the outward normal. Since we are assuming that the geometry and the flow are independent of x, we could set $x_0 = 0$ without loss of generality.

A full solution of (2.1a, b) would be formidably complicated. Aris (1956) showed that the x-derivatives could be eliminated if one only sought the first few moments

$$m^{(p)} = \int_{-\infty}^{\infty} (x-x_0)^p \bar{c}\, \mathrm{d}x \tag{2.2a}$$

and

$$b^{(p)} = \int_{-\infty}^{\infty} (x-x_0)^p (c-\bar{c})\, \mathrm{d}x \quad (p = 0, 1, 2, \ldots), \tag{2.2b}$$

where an overbar denotes the cross-sectional average value. Taking moments of (2.1a, b), we find that

$$m^{(0)} = \bar{q} \quad \text{for } t > t_0, \tag{2.3a}$$

$$m^{(p)} = p \int_{t_0}^{t} \overline{(u-\bar{u})\, b^{(p-1)}}\, \mathrm{d}t' + p(p-1) \int_{t_0}^{t} \bar{\kappa}_{11}\, m^{(p-2)}\, \mathrm{d}t' + p(p-1) \int_{t_0}^{t} \overline{(\kappa_{11}-\bar{\kappa}_{11})\, b^{(p-2)}}\, \mathrm{d}t' \tag{2.3b}$$

(Aris 1956, equation (12)), and that the zero-average terms b^p satisfy the equations

$$\begin{aligned} &\partial_t b^{(p)} - \nabla\cdot(\boldsymbol{\varkappa}\cdot\nabla b^{(p)}) \\ &\quad = p\{(u-\bar{u})\, m^{(p-1)} + (u-\bar{u})\, b^{(p-1)} - \overline{(u-\bar{u})\, b^{(p-1)}}\} \\ &\qquad + p(p-1)\{(\kappa_{11}-\bar{\kappa}_{11})\, m^{(p-2)} + \kappa_{11}\, b^{(p-2)} - \overline{\kappa_{11}\, b^{(p-2)}}\} \end{aligned} \tag{2.4a}$$

with

$$\boldsymbol{n}\cdot\boldsymbol{\varkappa}\cdot\nabla b^{(p)} = 0 \quad \text{on } \partial A \tag{2.4b}$$

and

$$b^{(0)} = q-\bar{q}, \quad b^{(1)} = b^{(2)} = \ldots = 0 \quad \text{at } t = t_0. \tag{2.4c}$$

Despite the more complicated looking right-hand-side forcing terms, the absence of x-derivatives means that the moment equations (2.3) and (2.4) are far more tractable than the full equations (2.1). Yet knowledge of just the zero, first and second moments gives us the area, centroid and variance, and so permits a Gaussian approximation to the concentration distribution along each line (y,z). Allen (1982) and Smith (1982) have established that for oscillatory flows the skewness with respect to x decays quite rapidly after the first half-cycle. Hence for oscillatory flows the Gaussian approximation is even more accurate than it is for steady flows.

3. The centroid-displacement functions

Following Smith (1981), we shall make the further simplification of only seeking asymptotic results valid at large times after discharge. If B denotes a typical breadthscale across the flow, then the timescale for the decay of any free transients in (2.4a–c) is of order

$$T_c = O(B^2/\bar{\kappa}_{22}). \tag{3.1}$$

In particular, for the zero moment $b^{(0)}$ there is no forcing term in (2.4a), so the response is completely free:

$$b^{(0)} \sim 0 \quad \text{for } t-t_0 \gg T_c. \tag{3.2}$$

Depending how wide the flow is, this uniform mixing could be achieved in a small fraction of an oscillation or in many flow cycles.

For $p = 1$, (2.4a) becomes

$$\partial_t b^{(1)} - \nabla\cdot(\boldsymbol{\varkappa}\cdot\nabla b^{(1)}) = (u-\overline{u})\,\overline{q} + (u-\overline{u})\,b^{(0)} - \overline{(u-\overline{u})\,b^{(0)}} \quad \text{for } t > t_0. \tag{3.3}$$

When the transient $b^{(0)}$ forcing has decayed away, the remaining $(u-\overline{u})\,\overline{q}$ forcing term gives rise to the asymptotic solution

$$b^{(1)} \sim b^{(1)}_\infty = \overline{q} g_+(y,z,t), \tag{3.4}$$

where the centroid-displacement function g_+ satisfies the transverse diffusion equation

$$\partial_t g_+ - \nabla\cdot(\boldsymbol{\varkappa}\cdot\nabla g_+) = u-\overline{u}, \tag{3.5a}$$

with

$$\boldsymbol{n}\cdot\boldsymbol{\varkappa}\cdot\nabla g_+ = 0 \quad \text{on } \partial A \tag{3.5b}$$

and

$$\overline{g}_+ = 0. \tag{3.5c}$$

In the work of Holley, Harleman & Fischer (1970, equations (2), (8)) the function g_+ arises in the representation of the concentration distribution

$$c = \overline{c} - g_+(y,z,t)\,\partial_x \overline{c} + \ldots.$$

Their equations (21) and (22) show that the phase of g_+ relative to the tidal current is sensitive to the ratio T/T_c between the timescale T of the flow oscillations and the mixing time T_c. In view of the strong dependence (3.1) of T_c upon the channel breadth B, the distinction between slow and fast oscillations amounts to a distinction between narrow and wide estuaries. The transition width is typically about 100 m. For narrow estuaries g_+ tends to be in phase with the current $\overline{u}(t)$, while for wide estuaries g_+ lags by up to quarter of a cycle behind the oscillatory current. This phase lag has profound implications as regards the character and efficiency of the dispersion process in oscillatory flows.

For $p = 1$, (2.3b) becomes

$$m^{(1)} = \int_{t_0}^{t} \overline{(u-\overline{u})\,b^{(0)}}\,\mathrm{d}t'. \tag{3.6}$$

At first sight it might seem that, to determine $m^{(1)}$ at large times after discharge, it would be necessary to know the full t-dependence of $b^{(0)}$. However, a modification of a mathematical device used by Smith (1984, Appendix A) enables us to get around this difficulty. Following the general procedure described in the Appendix to the present paper, we are led to introduce the auxiliary function g_-:

$$-\partial_t g_- - \nabla\cdot(\boldsymbol{\varkappa}\cdot\nabla g_-) = u-\overline{u}, \tag{3.7a}$$

with

$$\boldsymbol{n}\cdot\boldsymbol{\varkappa}\cdot\nabla g_- = 0 \quad \text{on } \partial A \tag{3.7b}$$

and

$$\overline{g}_- = 0. \tag{3.7c}$$

The result (A 5) leads immediately to an explicit formula for the integral:

$$\int_{t_0}^{t} \overline{(u-\overline{u})\,b^{(0)}}\,\mathrm{d}t' = \overline{g_-\,b^{(0)}}\big|_{t_0} - \overline{g_-\,b^{(0)}}\big|_{t}. \tag{3.8}$$

From the starting value (2.4c),

$$b^{(0)} = q - \overline{q} \quad \text{at } t = t_0, \tag{3.9}$$

and the asymptote (3.2), we infer that

$$m^{(1)} \sim \overline{g_- q}|_{t_0} \quad \text{for } t-t_0 \gg T_{\text{dec}}. \tag{3.10}$$

In axes moving with the bulk velocity $\bar{u}$, the centroid displacement $X(y,z,t)$ along the line (y,z) can be defined:

$$X = \frac{m^{(1)}+b^{(1)}}{m^{(0)}+b^{(0)}} \sim \frac{\overline{g_- q}|_{t_0}}{\bar{q}} + g_+(y,z,t). \tag{3.11}$$

Thus g_+ describes the cross-stream shifting of the centroid position, and g_- gives the long-term influence of the shape and timing of the discharge. For a point release at (y_0, z_0),

$$q = \bar{q}\delta(y-y_0)\,\delta(z-z_0), \tag{3.12}$$

the asymptotic centroid displacement has the symmetric form

$$X \sim g_-(y_0,z_0,t_0)+g_+(y,z,t). \tag{3.13}$$

For later use we note that, applying the analysis of the Appendix to the equations (3.5) and (3.7) for g_+ and g_-, we can deduce that for an arbitrary reference time t_*:

$$\int_{t_0}^{t_*} \overline{ug_+}\,\mathrm{d}t' - \overline{g_+ g_-}|_{t_0} = \int_{t_0}^{t_*} \overline{ug_-}\,\mathrm{d}t' - \overline{g_+ g_-}|_{t_*}. \tag{3.14}$$

4. The variance functions

For $p = 2$, (2.4a) becomes

$$\partial_t b^{(2)} - \nabla\cdot(\boldsymbol{\kappa}\cdot\nabla b^{(2)}) = 2m^{(1)}(u-\bar{u}) + 2\{(u-\bar{u})\,b^{(1)} - \overline{(u-\bar{u})\,b^{(1)}}\}$$
$$+ 2\bar{q}(\kappa_{11}-\bar{\kappa}_{11}) + 2\{\kappa_{11}\,b^{(0)} - \overline{\kappa_{11}\,b^{(0)}}\}. \tag{4.1}$$

At large times after discharge the $\kappa_{11}\,b^{(0)}$ forcing terms vanish. Corresponding to the three remaining groups of forcing terms, we decompose $b^{(2)}$ as

$$b^{(2)} \sim b_\infty^{(2)} = 2\overline{g_- q}\,g_+ + 2\bar{q}g_+^{(2)} + 2\bar{q}K_+. \tag{4.2}$$

Here the variance function $g_+^{(2)}$ and the diffusivity function K_+ satisfy the forced transverse diffusion equations

$$\partial_t g_+^{(2)} - \nabla\cdot(\boldsymbol{\kappa}\cdot\nabla g_+^{(2)}) = (u-\bar{u})\,g_+ - \overline{(u-\bar{u})\,g_+}, \tag{4.3a}$$

$$\partial_t K_+ - \nabla\cdot(\boldsymbol{\kappa}\cdot\nabla K_+) = \kappa_{11}-\bar{\kappa}_{11}, \tag{4.3b}$$

with
$$\boldsymbol{n}\cdot\boldsymbol{\kappa}\cdot\nabla g_+^{(2)} = \boldsymbol{n}\cdot\boldsymbol{\kappa}\cdot\nabla K_+ = 0 \quad \text{on } \partial A \tag{4.3c}$$

and
$$\overline{g_+^{(2)}} = \overline{K_+} = 0. \tag{4.3d}$$

For $p = 2$, (2.3b) becomes

$$m^{(2)} = 2\bar{q}\left\{\int_{t_0}^{t} \overline{(u-\bar{u})\,g_+}\,\mathrm{d}t' + \int_{t_0}^{t} \bar{\kappa}_{11}\,\mathrm{d}t'\right\}$$
$$+ 2\int_{t_0}^{t} \overline{(u-\bar{u})\,(b^{(1)}-b_\infty^{(1)})}\,\mathrm{d}t' + 2\int_{t_0}^{t} \overline{(\kappa_{11}-\bar{\kappa}_{11})\,b^{(0)}}\,\mathrm{d}t', \tag{4.4}$$

where we have made use of the formula (3.4) for $b_\infty^{(1)}$.

As was the case with equation (3.6) for $m^{(1)}$, it might appear that to evaluate $m^{(2)}$ it would be necessary to know the full t-dependence of both $b^{(0)}$ and $b^{(1)}-b_\infty^{(1)}$. Again

we adopt the procedure described in the Appendix to get around this difficulty. For the $\overline{(\kappa_{11}-\bar{\kappa}_{11})\,b^{(0)}}$ integral in (4.4) this is straightforward. By analogy with (3.7*a–c*), we introduce the auxiliary function K_-:

$$-\partial_t K_- - \boldsymbol{\nabla}\cdot(\boldsymbol{\varkappa}\cdot\boldsymbol{\nabla}K_-) = \kappa_{11}-\bar{\kappa}_{11}, \tag{4.5a}$$

with
$$\boldsymbol{n}\cdot\boldsymbol{\varkappa}\cdot\boldsymbol{\nabla}K_- = 0 \quad \text{on } \partial A \tag{4.5b}$$

and
$$\overline{K_-} = 0. \tag{4.5c}$$

The corresponding version of (A 5) is

$$\int_{t_0}^{t} \overline{(\kappa_{11}-\bar{\kappa}_{11})\,b^{(0)}}\,\mathrm{d}t' = \overline{K_- q}|_{t_0} - \overline{K_- b^{(0)}}|_t. \tag{4.6}$$

At large time after discharge the transient $\overline{K_- b^{(0)}}$ contribution decays away.

The $\overline{(u-\bar{u})\,(b^{(1)}-b_\infty^{(1)})}$ integral is a more formidable obstacle. First, we infer from (2.4), (3.4) and (3.5) that $b^{(1)}-b_\infty^{(1)}$ satisfies the diffusion equation

$$\partial_t(b^{(1)}-b_\infty^{(1)}) - \boldsymbol{\nabla}\cdot(\boldsymbol{\varkappa}\cdot\boldsymbol{\nabla}(b^{(1)}-b_\infty^{(1)})) = (u-\bar{u})\,b^{(0)} - \overline{(u-\bar{u})\,b^{(0)}}, \tag{4.7a}$$

with
$$\boldsymbol{n}\cdot\boldsymbol{\varkappa}\cdot\boldsymbol{\nabla}(b^{(1)}-b_\infty^{(1)}) = 0 \quad \text{on } \partial A \tag{4.7b}$$

and
$$b^{(1)}-b_\infty^{(1)} = -\bar{q}g_+ \quad \text{at } t = t_0. \tag{4.7c}$$

Thus, in the notation of the Appendix (equation (A 2*a*)), we have

$$s = (u-\bar{u})\,b^{(0)}. \tag{4.8}$$

Using the auxiliary function g_- in the formula (A 5), we obtain the representation

$$\int_{t_0}^{t} \overline{(u-\bar{u})\,(b^{(1)}-b_\infty^{(1)})}\,\mathrm{d}t' = -\overline{q\,g_-\,g_+}|_{t_0} - \overline{g_-(b^{(1)}-b_\infty^{(1)})}|_t + \int_{t_0}^{t} \overline{(u-\bar{u})\,b^{(0)}g_-}\,\mathrm{d}t'. \tag{4.9}$$

We remark that by definition $b^{(1)}-b_\infty^{(1)}$ is transient and decays away at large times after discharge.

As is noted in the Appendix, the representation (4.9) is not merely the replacement of one intractable integral by another. From (4.7*a*) we see that $(u-\bar{u})\,b^{(0)}$ can be regarded as being two spatial derivatives simpler than $b^{(1)}-b_\infty^{(1)}$. Encouraged by this observation, we rewrite the remaining integral in a manner suitable for the repeated use of the results of the Appendix:

$$\int_{t_0}^{t} \overline{(u-\bar{u})\,b^{(0)}g_-}\,\mathrm{d}t' = \int_{t_0}^{t} \overline{[(u-\bar{u})\,g_- - \overline{(u-\bar{u})\,g_-}]\,b^{(0)}}\,\mathrm{d}t'. \tag{4.10}$$

In the notation of the Appendix, this time we have

$$r = (u-\bar{u})\,g_-. \tag{4.11}$$

Hence the appropriate auxiliary function is $g_-^{(2)}$:

$$-\partial_t g_-^{(2)} - \boldsymbol{\nabla}\cdot(\boldsymbol{\varkappa}\cdot\boldsymbol{\nabla}g_-^{(2)}) = (u-\bar{u})\,g_- - \overline{(u-\bar{u})\,g_-}, \tag{4.12a}$$

with
$$\boldsymbol{n}\cdot\boldsymbol{\varkappa}\cdot\boldsymbol{\nabla}g_-^{(2)} = 0 \quad \text{on } \partial A \tag{4.12b}$$

and
$$\overline{g_-^{(2)}} = 0. \tag{4.12c}$$

This time the formula (A 5) gives us a closed-form representation

$$\int_{t_0}^{t} \overline{(r-\bar{r})\,b^{(0)}}\,\mathrm{d}t' = \overline{g_-^{(2)}\,q}|_{t_0} - \overline{g_-^{(2)}\,b^{(0)}}|_t. \tag{4.13}$$

The final asymptotic formula for $m^{(2)}$, based upon (4.6), (4.9) and (4.13), is

$$m^{(2)} \sim 2\bar{q}\left\{\int_{t_0}^{t} [\overline{ug_+}+\bar{\kappa}_{11}]\,dt' - \overline{g_+ g_-}|_{t_0}\right\} + 2\overline{g_-^{(2)} q}|_{t_0} + 2\overline{K_- q}|_{t_0}. \tag{4.14}$$

The variance $\sigma^2(y,z,t)$ along the line (y,z) is related to the second moment about the centroid $X(y,z,t)$:

$$\begin{aligned}\sigma^2 &= \frac{m^{(2)}+b^{(2)}}{m^{(0)}+b^{(0)}} - X^2 \sim \frac{m^{(2)}}{m^{(0)}} + \frac{b_\infty^{(2)}}{m^{(0)}} - X^2 \\ &\sim 2\left\{\int_{t_0}^{t} [\overline{ug_+}+\bar{\kappa}_{11}]\,dt' - \overline{g_+ g_-}|_{t_0}\right\} \\ &\quad + 2\frac{\overline{g_-^{(2)} q}|_{t_0}}{\bar{q}} - \left(\frac{\overline{g-q}}{\bar{q}}\right)^2_{t_0} + 2\frac{\overline{K_- q}|_{t_0}}{\bar{q}} + 2g_+^{(2)} - g_+^2 + 2K_+. \end{aligned} \tag{4.15}$$

This is the central result of this paper. We note that σ^2 depends on the time elapsed since discharge, the discharge shape q, and the precise position (y,z) at which the observations are made. In the Gaussian approximation the peak concentration varies as σ^{-1}. So the objective of low pollution levels becomes a quest for maximizing σ^2.

5. Definitions of the shear-dispersion coefficient

Conventionally analyses of contaminant dispersion have concerned the cross-sectionally averaged concentration $\bar{c}$ and the corresponding moments $m^{(p)}$. The asymptotic shear-dispersion coefficient D is defined by

$$\frac{d}{dt}\left(\frac{m^{(2)}}{m^{(0)}}\right) \sim 2(D+\bar{\kappa}_{11}), \quad \text{i.e.} \quad D = \overline{ug_+}. \tag{5.1}$$

(In practice D is usually much larger than the longitudinal-mixing contribution $\bar{\kappa}_{11}$ to the spreading rate.) Chatwin (1975) drew attention to the fact that D is not always positive. In many situations the contaminant cloud appears to be periodically expanding and contracting (Holley, Harleman & Fischer 1970, figure 4). This leads to conceptual difficulties when D is regarded as an effective diffusion coefficient (Smith 1982).

Yasuda (1982) points out that much of the apparent contraction of the contaminant cloud is simply due to the relative movement between the faster- and slower-moving parts of the flow. This relative movement is factored out in the definition of the variance $\sigma^2(y,z,t)$ along each line (y,z). Thus he advocated that the shear-dispersion coefficient should be defined by

$$\frac{d}{dt}\overline{\sigma^2} \sim 2(\tilde{D}+\bar{\kappa}_{11}). \tag{5.2}$$

For the particular case that he studied, Yasuda found numerically that, unlike D, the alternative definition $\tilde{D}$ did remain positive.

Our analytic expression (4.15) for $\sigma^2(y,z,t)$, together with the equations (3.5) and (4.3) satisfied by g_+, $g_+^{(2)}$ and K_+, permits us to derive the forced diffusion equation

$$\partial_t \sigma^2 - \nabla\cdot(\boldsymbol{\kappa}\cdot\nabla\sigma^2) \sim 2\kappa_{11} + 2\nabla g_+ \cdot \boldsymbol{\kappa}\cdot\nabla g_+, \tag{5.3a}$$

with

$$\boldsymbol{n}\cdot\boldsymbol{\kappa}\cdot\nabla\sigma^2 = 0 \quad \text{on } \partial A. \tag{5.3b}$$

Taking the cross-sectional average, we obtain

$$\frac{\mathrm{d}}{\mathrm{d}t}\overline{\sigma^2} \sim 2(\bar{\kappa}_{11}+\overline{\nabla g_+ \cdot \boldsymbol{\kappa} \cdot \nabla g_+}), \quad \text{i.e. } \tilde{D} = \overline{\nabla g_+ \cdot \boldsymbol{\kappa} \cdot \nabla g_+}. \tag{5.3c}$$

This analytic expression confirms that $\tilde{D}$ is indeed non-negative. Even though there can be contraction at some positions across the flow (Smith 1983), on average σ^2 is increasing.

The relationship between D and $\tilde{D}$ can be ascertained by multiplying the equation (3.5*a*) for g_+ by g_+, and integrating across the flow:

$$D = \tilde{D} + \frac{1}{2}\frac{\mathrm{d}}{\mathrm{d}t}(\overline{g_+^2}). \tag{5.4}$$

It is when the relative centroid displacement g_+ is large and rapidly changing that negative values of D can arise. When averaged over a flow cycle the two definitions of the shear dispersion coefficient are equivalent:

$$\langle D \rangle = \langle \tilde{D} \rangle, \tag{5.5}$$

where the angle brackets $\langle \ldots \rangle$ indicate averages over a flow cycle.

6. When to make a uniform discharge

Relative to the systematic long-term growth of the variance, the excess variance $\delta\sigma^2$, associated with the precise discharge and observation conditions, can be defined as

$$\delta\sigma^2 = \sigma^2 - 2\delta t[\langle D \rangle + \langle \bar{\kappa}_{11} \rangle], \tag{6.1a}$$

with

$$\delta t = t - t_0. \tag{6.1b}$$

To emphasize the division of $\delta\sigma^2$ into discharge and observation terms, we choose an arbitrary but fixed reference time t_*, and using the relationship (3.14) we rewrite the key result (4.15):

$$\begin{aligned}\delta\sigma^2 \sim{}& 2\int_{t_0}^{t_*} [\overline{ug_-} - \langle D \rangle + \bar{\kappa}_{11} - \langle \bar{\kappa}_{11} \rangle]\,\mathrm{d}t' + 2\frac{\overline{g_-^{(2)} q}|_{t_0}}{\bar{q}} - \left(\frac{\overline{g_- q}}{\bar{q}}\right)^2_{t_0} \\ &+ 2\frac{\overline{K_- q}|_{t_0}}{\bar{q}} - 2\overline{g_- g_+}|_{t_*} + 2\int_{t_*}^{t} [\overline{ug_+} - \langle D \rangle + \bar{\kappa}_{11} - \langle \bar{\kappa}_{11} \rangle]\,\mathrm{d}t' \\ &+ 2g_+^{(2)}(y,z,t) - g_+(y,z,t)^2 + 2K_+(y,z,t).\end{aligned} \tag{6.2}$$

If we neither know where nor how long after discharge the pollution will be experienced, then the best that we can do is to ensure that on average $\delta\sigma^2$ is as large as possible. Averaging with respect to (y,z,t), we find from (6.2 and (5.4) that

$$\begin{aligned}\langle \overline{\delta\sigma^2} \rangle = {}& 2\int_{t_0}^{t_*} [\overline{ug_-} - \langle D \rangle + \bar{\kappa}_{11} - \langle \bar{\kappa}_{11} \rangle]\,\mathrm{d}t' + 2\frac{\overline{g_-^{(2)} q}|_{t_0}}{\bar{q}} - \left(\frac{\overline{g_- q}}{\bar{q}}\right)^2_{t_0} + 2\frac{\overline{K_- q}|_{t_0}}{\bar{q}} \\ &- 2\overline{g_+ g_-}|_{t_*} - \overline{g_+^2}|_{t_*} + 2\int_{t_*}^{\hat{t}} [\tilde{D} - \langle D \rangle + \bar{\kappa}_{11} - \langle \bar{\kappa}_{11} \rangle]\,\mathrm{d}t',\end{aligned} \tag{6.3}$$

where $\hat{t}$ is the first time after t_* that the final integrand is zero.

For a uniform discharge $q = \bar{q}$ it follows from (6.3) that

$$\frac{\mathrm{d}}{\mathrm{d}t_0}\langle \overline{\delta\sigma^2} \rangle = 2[\langle D \rangle + \langle \bar{\kappa}_{11} \rangle - \overline{ug_-} - \bar{\kappa}_{11}]. \tag{6.4}$$

Hence to maximize $\langle\overline{\delta\sigma^2}\rangle$ the discharge time t_0 should be chosen when

$$\overline{ug_-}+\overline{\kappa}_{11} = \langle D\rangle+\langle\overline{\kappa}_{11}\rangle. \tag{6.5}$$

Since in practice $\langle D\rangle$ is much larger than $\langle\overline{\kappa}_{11}\rangle$, the optimal timing t_0 for a uniform discharge is when $\overline{ug_-}$ rises to the value $\langle D\rangle$.

For a particular flow with a $\sin\omega t$ velocity field and with $\boldsymbol{\varkappa}$ constant, Smith (1983, equation (6.6)) deduced that for a uniform discharge the optimal timing varied from $\omega t_0 = \frac{1}{4}\pi$ for rapid mixing, to $\omega t_0 = 0$ for slow mixing. The present analysis enables us to reveal the generality of those deductions. For narrow flows with rapid mixing g_- is almost in phase with the current, so

$$\overline{ug_-} = 2\langle D\rangle \sin^2\omega t \tag{6.6}$$

(Bowden 1965). Hence the optimal timing for a uniform discharge is $\omega t_0 = \frac{1}{4}\pi$. In the opposite limit, of wide flows with slow mixing, g_- leads the current by $\frac{1}{2}\pi$:

$$\overline{ug_-} = E\sin 2\omega t+2\langle D\rangle\sin^2\omega t, \quad \text{with } E \gg \langle D\rangle \tag{6.7}$$

(Chatwin 1975). Thus the optimal timing is soon after $\omega t_0 = 0$. The relatively small value of $\langle D\rangle$ makes the variance particularly sensitive to the discharge timing in this wide-flow limit.

7. When and where to make a point discharge

For an instantaneous point discharge

$$q = \bar{q}\delta(y-y_0)\,\delta(z-z_0) \quad \text{at } t = t_0 \tag{7.1}$$

the averaged excess variance $\langle\overline{\delta\sigma^2}\rangle$ depends upon the discharge location (y_0, z_0) as well as upon the timing t_0. Instead of the ordinary differential equation (6.4), we find (making use of the equations (3.7), (4.12) and (4.5) satisfied by g_-, $g^{(2)}$ and K_-) that $\langle\overline{\delta\sigma^2}\rangle$ satisfies the time-reversed diffusion equation

$$-\partial_{t_0}\langle\overline{\delta\sigma^2}\rangle-\boldsymbol{\nabla}_0\cdot(\boldsymbol{\varkappa}\cdot\boldsymbol{\nabla}_0\langle\overline{\delta\sigma^2}\rangle) = 2(\kappa_{11}-\langle\overline{\kappa}_{11}\rangle)+2[\boldsymbol{\nabla}_0 g_-\cdot\boldsymbol{\varkappa}\cdot\boldsymbol{\nabla}_0 g_--\langle D\rangle], \tag{7.2a}$$

with

$$\boldsymbol{n}\cdot\boldsymbol{\varkappa}\cdot\boldsymbol{\nabla}_0\langle\overline{\delta\sigma^2}\rangle = 0 \quad \text{on } \partial A. \tag{7.2b}$$

The time-reversed character of (7.2a) means that the long-term influence of the discharge conditions depends only upon what happens *after* the discharge has taken place. Since shear dispersion generally dominates longitudinal mixing, the source term in (7.2a) is effectively

$$2[d_--\langle\bar{d}_-\rangle], \quad \text{with} \quad d_- = \boldsymbol{\nabla}_0 g_-\cdot\boldsymbol{\varkappa}\cdot\boldsymbol{\nabla}_0 g_-, \tag{7.3a,b}$$

Where d_- can be thought of as a local, time-reversed counterpart to the dispersion coefficient D.

When mixing is rapid $\langle\overline{\delta\sigma^2}\rangle$ is predominantly a function of time:

$$-\partial_{t_0}\langle\overline{\delta\sigma^2}\rangle = 2[\bar{d}_--\langle\bar{d}_-\rangle]. \tag{7.4}$$

By analogy with (6.4) and (6.5), we infer that the optimal timing is when $\bar{d}_--\langle\bar{d}_-\rangle$ changes sign from negative to positive as t_0 increases, i.e.

$$\bar{d}_- = \overline{\boldsymbol{\nabla}_0 g_-\cdot\boldsymbol{\varkappa}\cdot\boldsymbol{\nabla}_0 g_-} \quad \text{rises to} \quad \langle\bar{d}_-\rangle = \langle D\rangle. \tag{7.5}$$

For a $\sin\omega t$ velocity field with $\boldsymbol{\varkappa}$ independent of time, this optimal discharge timing for narrow flows is at $\omega t_0 = \frac{1}{4}\pi$ (as was also the case for a uniform discharge). The

residual dependence of $\langle\overline{\delta\sigma^2}\rangle$ upon the precise cross-stream position of the discharge is given by the transverse diffusion equation

$$-\nabla_0\cdot(\varkappa\cdot\nabla\langle\overline{\delta\sigma^2}\rangle) = 2[d_- - \bar{d}_-]. \tag{7.6}$$

Hence the best position tends to be in a region where d_- is relatively large.

In the opposite limit, of slow mixing, $\langle\overline{\delta\sigma^2}\rangle$ is predominantly a function of the discharge position across the flow:

$$-\nabla_0\cdot(\langle\varkappa\rangle\cdot\nabla_0\langle\overline{\delta\sigma^2}\rangle) = 2(\langle d_-\rangle - \langle\bar{d}_-\rangle]. \tag{7.7}$$

Hence the best position is again in a region where d_- is relatively large. If we assume that the shape of $\varkappa$ remains self-similar throughout the flow oscillations, then the residual t_0 dependence of $\langle\overline{\delta\sigma^2}\rangle$ is given by

$$-\partial_{t_0}\langle\overline{\delta\sigma^2}\rangle = 2[d_- - \langle d_-\rangle] - 2\left(\frac{\varkappa-\langle\varkappa\rangle}{\langle\varkappa\rangle}\right)[\langle d_-\rangle - \langle\bar{d}_-\rangle]. \tag{7.8}$$

Thus the optimal timing is then when

$$\frac{d_- - \langle d_-\rangle}{\langle d_-\rangle - \langle\bar{d}_-\rangle} \quad \text{overtakes} \quad \frac{\varkappa-\langle\varkappa\rangle}{\langle\varkappa\rangle}, \tag{7.9}$$

with (y_0, z_0) having the optimal values determined from (7.8). For a wide, $\sin\omega t$ velocity field with $\varkappa$ independent of time, d_- varies as $\cos^2\omega t_0$. Hence the optimal timing arises at $\omega t_0 = \frac{3}{4}\pi$, i.e. before flow reversal. This is earlier than for a uniform discharge. A physical explanation is that for a point discharge it takes time to diffuse across the flow and to take advantage of the large relative displacements g_+ between the faster- and slower-moving parts of the flow. To compensate, the point discharge has to be that much earlier.

If there is an axis of symmetry then $\nabla_0 g_- = 0$, and the local time-reversed dispersion coefficient d_- is zero. Similarly, at the banks we have

$$\boldsymbol{n}\cdot\varkappa\cdot\nabla_0 g_- = 0 \quad \text{on } \partial A, \tag{7.10}$$

and d_- is again zero. In the two limiting cases, of rapid and of slow mixing, we have just ascertained that the best position tends to be in a region where d_- is relatively large. Thus in an oscillatory flow the optimal location for a discharge will be away from the centre or the sides. This is unlike the situation for steady flows (Smith 1981, 1984; Daish 1985), where the low velocity in the shallow water gives extra time for shear dispersion (at the large asymptotic rate), which more than compensates for the initially weak dispersion close to the discharge. When the flow is oscillatory the contaminant is swept back and forth along the channel, so any time advantage is annulled.

An important practical point is that real discharges are not passive. Near-field momentum and buoyancy effects tend to augment the transverse mixing. Thus the actual contaminant cloud will be wider than a passive cloud, and the effective time of discharge is earlier than the actual discharge time. Correspondingly the optimal discharge time will tend to be slightly later than calculated here for passive discharges.

8. Shallow estuaries

In order to illustrate the general results derived in §§5–7, we seek a problem that is not unduly complicated, but is nevertheless of interest in its own right. The chosen problem is contaminant dispersion in a vertically well-mixed estuary of parabolic cross-section.

For unstratified water less than 20 m deep, vertical mixing takes place more rapidly than the tidal oscillations. In such shallow water the dominant long-term dispersion mechanism is associated with the lateral shear (Fischer 1972). Thus in applying the above analysis we can neglect the longitudinal turbulence contributions $\overline{\kappa}_{11}$, K_+ and K_-, and we can ignore any vertical concentration gradients. The water depth $h(y)$ enters the equation because it relates to the area over which lateral diffusion can take place. For example, the vertically integrated version of the equations (3.5) for the centroid displacement function $g_+(y,t)$ is

$$h\,\partial_t g_+ - \partial_y(h\,\|\kappa_{22}\|\,\partial_y g_+) = h(\|u\| - \overline{u}), \tag{8.1a}$$

with

$$h\,\|\kappa_{22}\|\,\partial_y g_+ = 0 \quad \text{on } y = y_R,\ y_L, \tag{8.1b}$$

and

$$0 = \overline{g_+} = \frac{\int_{y_R}^{y_L} h g_+ \,\mathrm{d}y}{\int_{y_R}^{y_L} h \,\mathrm{d}y}. \tag{8.1c}$$

Here $\|\ldots\|$ indicates a vertical-average value, and y_R and y_L are the positions of the right and left banks of the estuary. In regarding the estuary geometry as being independent of x, it is implicit that the tidal excursions are short compared with the estuary length.

With an eye towards algebraic simplicity, we follow Fischer (1972) and Smith (1983) by choosing the following flow and topography models:

$$\left.\begin{aligned} \|u\| &= \tfrac{5}{4}\overline{u}\left[1-\left(\frac{y}{B}\right)^2\right], \quad \|\kappa_{22}\| = k_2|\overline{u}|\,H\left[1-\left(\frac{y}{B}\right)^2\right], \\ h &= H\left[1-\left(\frac{y}{B}\right)^2\right], \quad y_R = -B, \quad y_L = B. \end{aligned}\right\} \tag{8.2}$$

Thus the local velocity and the transverse diffusivity are proportional to the local water depth, and the depth profile is parabolic. The empirical constant k_2 relating the turbulence to the bulk flow $\overline{u}$ is about 0.02.

The algebraic simplicity of the model (8.2) is revealed when we seek the solution of (8.1) for g_+. Just a single polynomial eigenmode is involved:

$$g_+ = \frac{1}{4}\left[1-5\left(\frac{y}{B}\right)^2\right] F_+(t), \tag{8.3a}$$

where the centroid-displacement factor F_+ satisfies the linear first-order differential equation

$$\frac{\mathrm{d}F_+}{\mathrm{d}t} + \frac{10k_2 H|\overline{u}|}{B^2}F_+ = \overline{u}(t). \tag{8.3b}$$

At first sight it might appear that the time dependence of $\varkappa$ (i.e. the $|\overline{u}|$ coefficient) complicates the solution of (8.3b). However, following Smith (1982, equation (3.5)), we can introduce an effective time coordinate

$$\tau = \frac{1}{\langle|\overline{u}|\rangle}\int_0^t |\overline{u}(t')|\,\mathrm{d}t'. \tag{8.4}$$

This transforms (8.3b) to the constant-coefficient form

$$\frac{\mathrm{d}F_+}{\mathrm{d}\tau} + \frac{F_+}{T_c} = \langle|\overline{u}|\rangle\,\mathrm{sgn}\,(\overline{u}), \tag{8.5a}$$

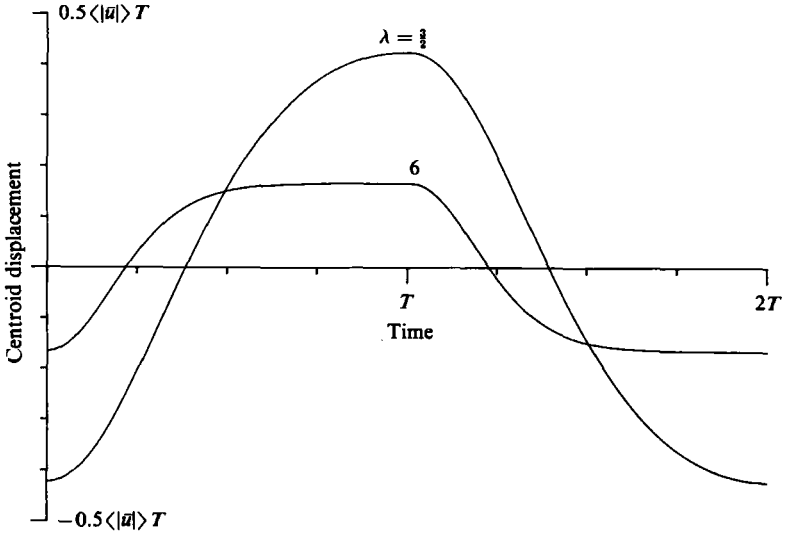

FIGURE 1. Centroid-displacement factors F_+ for a sinusoidal flow in a shallow estuary of parabolic cross-section. The two values $\lambda = \frac{3}{2}$ and 6 of the non-dimensional mixing rate are representative of wide and of narrow estuaries respectively.

with
$$T_c = \frac{B^2}{10k_2\langle|\overline{u}|\rangle}, \tag{8.5b}$$

where T_c is the timescale for mixing across the estuary. Hence the realism of time-dependent $\varkappa$ is achieved without the expected cost of mathematical complications.

In shallow estuaries the velocity profile can be markedly non-sinusoidal (Kreiss 1957). However, if the tide dominates the mean flow, then the volume fluxes associated with the ebb and flood are equal and opposite. Thus, with respect to τ there are equal spans of positive and negative $\overline{u}$:

$$\operatorname{sgn}(\overline{u}) = (-1)^n \quad \text{for } nT < \tau < (n+1)T, \tag{8.6}$$

where $2T$ is the wave period. The corresponding solution for the centroid-displacement factor is

$$F_+ = \langle|\overline{u}|\rangle T\frac{(-1)^n}{\lambda}\left\{1-\frac{2\exp(-\lambda\xi)}{1+\exp(-\lambda)}\right\}, \tag{8.7a}$$

with
$$\xi = \frac{\tau - nT}{T}, \quad \lambda = \frac{T}{T_c} = \frac{10k_2H\langle|\overline{u}|\rangle T}{B^2}. \tag{8.7b,c}$$

The use of T rather than π/ω avoids a profusion of π-factors in the subsequent formulae.

The parameter λ is a measure of the diffusive response rate in a flow period. For example, with $T = 2.1\times10^4$ s, $H = 10$ m, $\langle|\overline{u}|\rangle = 0.5$ m s^{-1},

$$\lambda = \left(\frac{145}{B}\right)^2. \tag{8.8}$$

We find below that the transition of behaviour between rapid and slow diffusive response occurs for $\lambda \sim 3$. Thus the dividing line between narrow and wide estuaries can be taken to be $B \sim 80$ m.

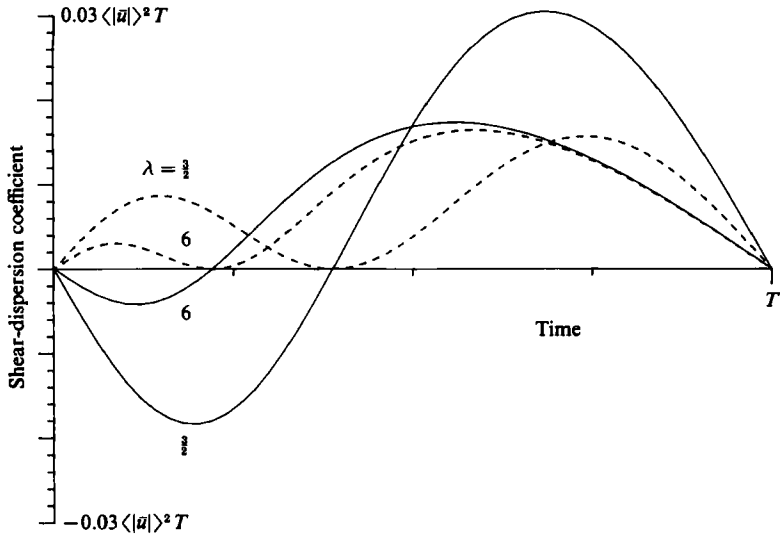

FIGURE 2. Comparison between the conventional D (——) and Yasuda's (1982) alternative definition $\tilde{D}$ (– – – –) of the shear-dispersion coefficient for a shallow estuary of parabolic cross-section with a sinusoidal flow.

Figure 1 shows the centroid displacement $F_+(t)$ for the particular case of a sinusoidal flow, i.e.

$$\bar{u} = \frac{\pi}{2}\langle|\bar{u}|\rangle \sin\frac{\pi t}{T}, \quad \xi = \frac{1}{2}\left(1-\cos\frac{\pi t}{T}\right). \tag{8.9}$$

For large λ (narrow estuaries) F_+ is approximately a square wave with only a small time lag behind the changing direction of the bulk flow $\bar{u}(t)$. In contrast, for small λ (wide estuaries) F_+ is almost exactly out of phase with the current.

The conventional definition (5.1) of the shear-dispersion coefficient is given by

$$D = \overline{ug_+} = \tfrac{1}{14}\bar{u}F_+ = \frac{|\bar{u}|\langle|\bar{u}|\rangle T}{14\lambda}\left\{1-\frac{2\exp(-\lambda\xi)}{1+\exp(-\lambda)}\right\}. \tag{8.10}$$

This is shown in figure 2 for the special case of sinusoidal flow. In keeping with the work of Chatwin (1975), we find that even for fairly large values of λ there can be a substantial timespan after flow reversal in which D is negative. The alternative definition (5.4) yields instead the strictly positive expression

$$\tilde{D} = \overline{\kappa_{22}(\nabla g_+)^2} = \frac{5}{7}\frac{k_2 H}{B^2}F_+^2|\bar{u}| = \frac{|\bar{u}|\langle|\bar{u}|\rangle T}{14\lambda}\left\{1-\frac{2\exp(-\lambda\xi)}{1+\exp(-\lambda)}\right\}^2. \tag{8.11}$$

Figure 2 reveals that for small λ (i.e. when the estuary is wide) there is a considerable difference between D and $\tilde{D}$.

The tidal-average values of D and $\tilde{D}$ are the same, and do not depend upon the detailed velocity profile $\bar{u}(t)$:

$$\langle D\rangle = \langle\tilde{D}\rangle = \frac{\langle|\bar{u}|\rangle^2 T}{14\lambda}\left\{1-\frac{2}{\lambda}\tanh\tfrac{1}{2}\lambda\right\} \tag{8.12a}$$

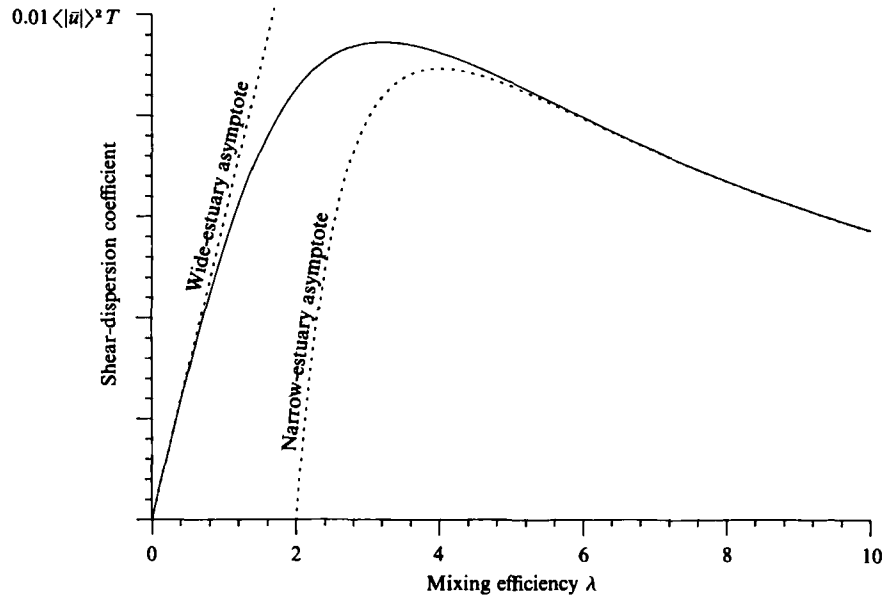

FIGURE 3. The tidally averaged dispersion coefficient for a parabolic estuary as a function of the mixing efficiency. The dotted curves give the wide- and narrow-estuary asymptotes.

(see figure 3). We remark that for the particular specification (8.8) the peak value of $\langle D\rangle$ is 50 m^2 s^{-1} at $B = 81$ m. The asymptotic forms for small and for large λ are

$$\langle D\rangle \sim \frac{\langle|\bar{u}|\rangle^2 T}{14}\tfrac{1}{12}\lambda, \quad \langle D\rangle \sim \frac{\langle|\bar{u}|\rangle^2 T}{14}\left(\frac{1}{\lambda}-\frac{2}{\lambda^2}\right). \tag{8.12b,c}$$

As was commented upon earlier, the transition of behaviour occurs for $\lambda \sim 3$.

For the influence function g_- associated with the discharge conditions, the counterpart of (8.3*a*) is

$$g_- = \frac{1}{4}\left[1-5\left(\frac{y}{B}\right)^2\right] F_-(t). \tag{8.13a}$$

Again, the use of the effective time coordinate τ leads to a constant-coefficient equation:

$$-\frac{\mathrm{d}F_-}{\mathrm{d}\tau}+\frac{F_-}{T_c} = \langle|\bar{u}|\rangle \operatorname{sgn}(\bar{u}). \tag{8.13b}$$

In the tidally dominated case the solution is

$$F_- = \langle|\bar{u}|\rangle T\frac{(-1)^n}{\lambda}\left\{1-\frac{2\exp(\lambda\xi-\lambda)}{1+\exp(-\lambda)}\right\}. \tag{8.13c}$$

For the particular case of sinusoidal flow, the solution for F corresponds to viewing figure 1 from the top of the page.

The counterpart of equation (8.10) for D is

$$\overline{ug_-} \approx \frac{|\bar{u}|\langle|\bar{u}|\rangle T}{14\lambda}\left\{1-\frac{2\exp(\lambda\xi-\lambda)}{1+\exp(-\lambda)}\right\}. \tag{8.14}$$

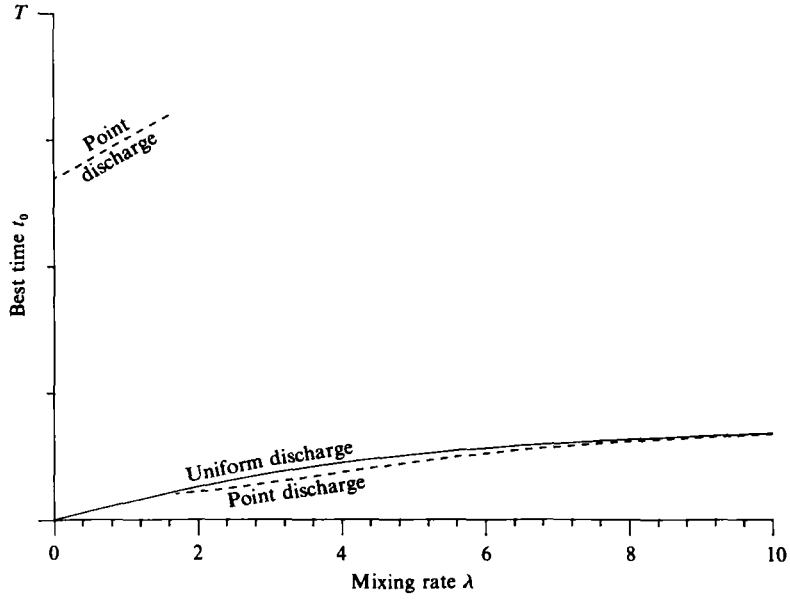

FIGURE 4. The optimal timing for uniform (——) and for point discharges (– – – –) in a shallow parabolic estuary with a sinusoidal flow.

For a sinusoidal flow $|\bar{u}|$ is symmetric about $t = 0$. Thus we can infer that the graph of $\overline{ug}_-$ is the reflection about $t = 0$ of the D-profile shown in figure 2. Since the optimal timing (6.5) for a uniform discharge is associated with a rising value of $\overline{ug}_-$, we deduce from figure 2 that the timing is soon after flow reversal. Using the results (8.12) and (8.14) in (6.5), we find that the optimal timing for a uniform discharge is when

$$\frac{|\bar{u}|}{\langle|\bar{u}|\rangle}\left\{1-\frac{2\exp(\lambda\xi_0-\lambda)}{1+\exp(-\lambda)}\right\} = 1-\frac{2}{\lambda}\tanh\tfrac{1}{2}\lambda. \tag{8.15a}$$

In the limits of strong and of weak mixing this becomes

$$\frac{|\bar{u}|}{\langle|\bar{u}|\rangle} \sim 1-\frac{2}{\lambda}, \quad \frac{|\bar{u}|}{\langle|\bar{u}|\rangle} \sim \tfrac{1}{6}\lambda. \tag{8.15b,c}$$

Thus, as was the case for κ_{22} independent of t (Smith 1983, equation (6.6)), the optimal timing is earlier when the estuary is wider. Figure 4 gives the timing for uniform discharges in a sinusoidal flow.

For point discharges the analysis of §7 requires us to consider the quantity d_- and its various averages:

$$d_- = \frac{|\bar{u}|\langle|\bar{u}|\rangle T}{\lambda}\frac{5}{8}\left(\frac{y}{B}\right)^2\left[1-\left(\frac{y}{B}\right)^2\right]\left\{1-\frac{2\exp(\lambda\xi_0-\lambda)}{1+\exp(-\lambda)}\right\}^2, \tag{8.16a}$$

$$\bar{d}_- = \frac{|\bar{u}|\langle|\bar{u}|\rangle T}{\lambda}\frac{1}{14}\left\{1-\frac{2\exp(\lambda\xi_0-\lambda)}{1+\exp(-\lambda)}\right\}^2, \tag{8.16b}$$

$$\langle d_-\rangle = \frac{\langle|\bar{u}|\rangle^2 T}{\lambda}\frac{5}{8}\left(\frac{y}{B}\right)^2\left[1-\left(\frac{y}{B}\right)^2\right]\left\{1-\frac{2}{\lambda}\tanh\tfrac{1}{2}\lambda\right\}, \tag{8.16c}$$

$$\langle\bar{d}_-\rangle = \frac{\langle|\bar{u}|\rangle^2 T}{\lambda}\frac{1}{14}\left\{1-\frac{2}{\lambda}\tanh\tfrac{1}{2}\lambda\right\}. \tag{8.16d}$$

Conveniently, the forcing terms $d_- - \bar{d}_-$ and $\langle d_- \rangle - \langle \bar{d}_- \rangle$ in (7.6) and (7.7) have the same y-dependence. After a straightforward calculation, we find that in both the limits of strong and of weak mixing the averaged excess variance $\langle \overline{\delta\sigma^2} \rangle$ has the shape

$$\text{constant} - 8\left(\frac{y_0}{B}\right)^2 + 5\left(\frac{y_0}{B}\right)^4 \tag{8.17}$$

with a maximum value along

$$\frac{y_0}{B} = (\tfrac{4}{5})^{\frac{1}{2}} = 0.894. \tag{8.18}$$

In the strong-mixing limit (7.5) yields the same timing as (8.15*b*). Along the optimal line the small-λ limit of (7.9) is

$$21\left\{\frac{|\bar{u}|}{\langle |\bar{u}| \rangle}(\tfrac{1}{2} - \xi_0)^2 - \tfrac{1}{12}\right\} \quad \text{overtakes} \quad \frac{|\bar{u}|}{\langle |\bar{u}| \rangle} - 1, \tag{8.19a}$$

i.e.

$$\xi_0 = \frac{1}{2} \pm \left\{\frac{1}{21} + \frac{1}{28}\frac{\langle |\bar{u}| \rangle}{|\bar{u}|}\right\}^{\frac{1}{2}}. \tag{8.19b}$$

For a sinusoidal flow the appropriate root is at

$$\xi_0 = t_0/T = 0.68, \tag{8.20}$$

i.e. displaced back to before flow reversal. We remark that the dip in value of $\varkappa$ (and hence of d_-) near flow reversal gives rise to a small local maximum of $\langle \overline{\delta\sigma^2} \rangle$ at $\xi_0 = 0.036$.

The vertically integrated version of (4.3*a*) is

$$h\,\partial_t g_+^{(2)} - \partial_y(h\,\|\kappa_{22}\|\,\partial_y g_+^{(2)}) = h[(\|u\| - \bar{u})\,g_+ - \overline{(\|u\| - \bar{u})\,g_+}], \tag{8.21a}$$

with

$$h\,\|\kappa_{22}\|\,\partial_y g_+^{(2)} = 0 \quad \text{on } y = y_R, y_L, \tag{8.21b}$$

and

$$\int_{y_R}^{y_L} h g_+^{(2)}\,\mathrm{d}y = 0. \tag{8.21c}$$

For the particular flow and topography model (8.2) the solution for $g_+^{(2)}$ involves two polynomial eigenmodes:

$$g_+^{(2)} = -\frac{1}{12}\left[1 - 5\left(\frac{y}{B}\right)^2\right] F_+^{(2)}(t) + \frac{25}{336}\left[1 - 14\left(\frac{y}{B}\right)^2 + 21\left(\frac{y}{B}\right)^4\right] E_+^{(2)}(t), \tag{8.22a}$$

with

$$\frac{\mathrm{d}F_+^{(2)}}{\mathrm{d}t} + \frac{10k_2 H|\bar{u}|}{B^2} F_+^{(2)} = F_+\,\bar{u}, \tag{8.22b}$$

$$\frac{\mathrm{d}E_+^{(2)}}{\mathrm{d}t} + \frac{28k_2 H|\bar{u}|}{B^2} E_+^{(2)} = F_+\,\bar{u}. \tag{8.22c}$$

In the tidally dominated case we can again use the effective time coordinate (8.4*a*) to derive explicit solutions for the modal amplitudes $F_+^{(2)}$ and $E_+^{(2)}$:

$$F_+^{(2)} = \frac{\langle |\bar{u}| \rangle^2 T^2}{\lambda^2} - \frac{2\langle |\bar{u}| \rangle^2 T^2 \exp(-\lambda\xi)}{\lambda(1 + \exp(-\lambda))}\left\{\xi + \frac{\exp(-\lambda)}{1 - \exp(-\lambda)}\right\}, \tag{8.23a}$$

$$E_+^{(2)} = \frac{\langle |\bar{u}| \rangle^2 T^2}{\mu\lambda} - \frac{2\langle |\bar{u}| \rangle^2 T^2}{\lambda(\mu - \lambda)(1 + \exp(-\lambda))}\left\{\exp(-\lambda\xi) - \frac{1 - \exp(-\lambda)}{1 - \exp(-\mu)}\exp(-\mu\xi)\right\}, \tag{8.23b}$$

with

$$\mu = \tfrac{14}{5}\lambda = \frac{28k_2 H\langle |\bar{u}| \rangle T}{B^2}. \tag{8.23c}$$

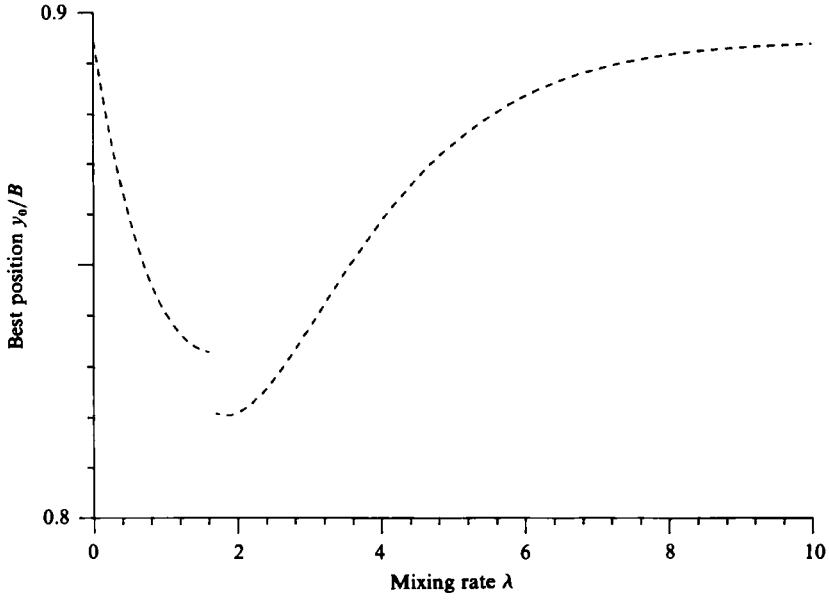

FIGURE 5. The best discharge site in a shallow parabolic estuary with a sinusoidal flow.

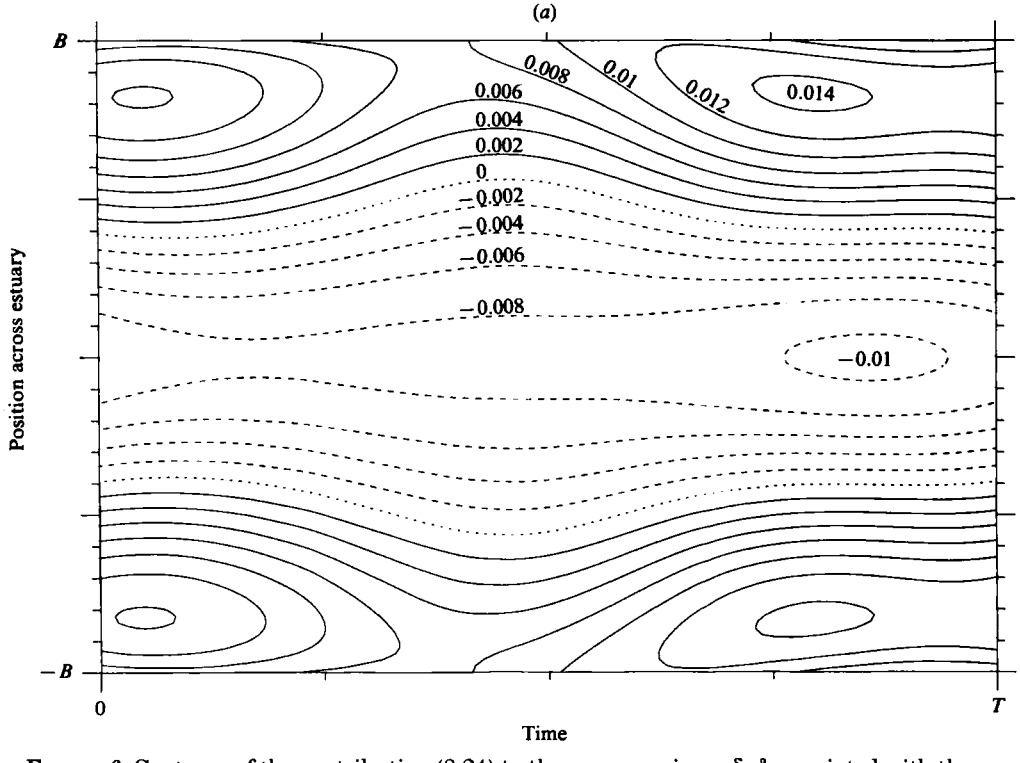

FIGURE 6. Contours of the contribution (8.24) to the excess variance $\delta\sigma^2$ associated with the precise timing and siting of a contaminant release. The non-dimensional mixing rates are (*a*) $\lambda = \frac{3}{2}$, (*b*) 3 and (*c*) 6.

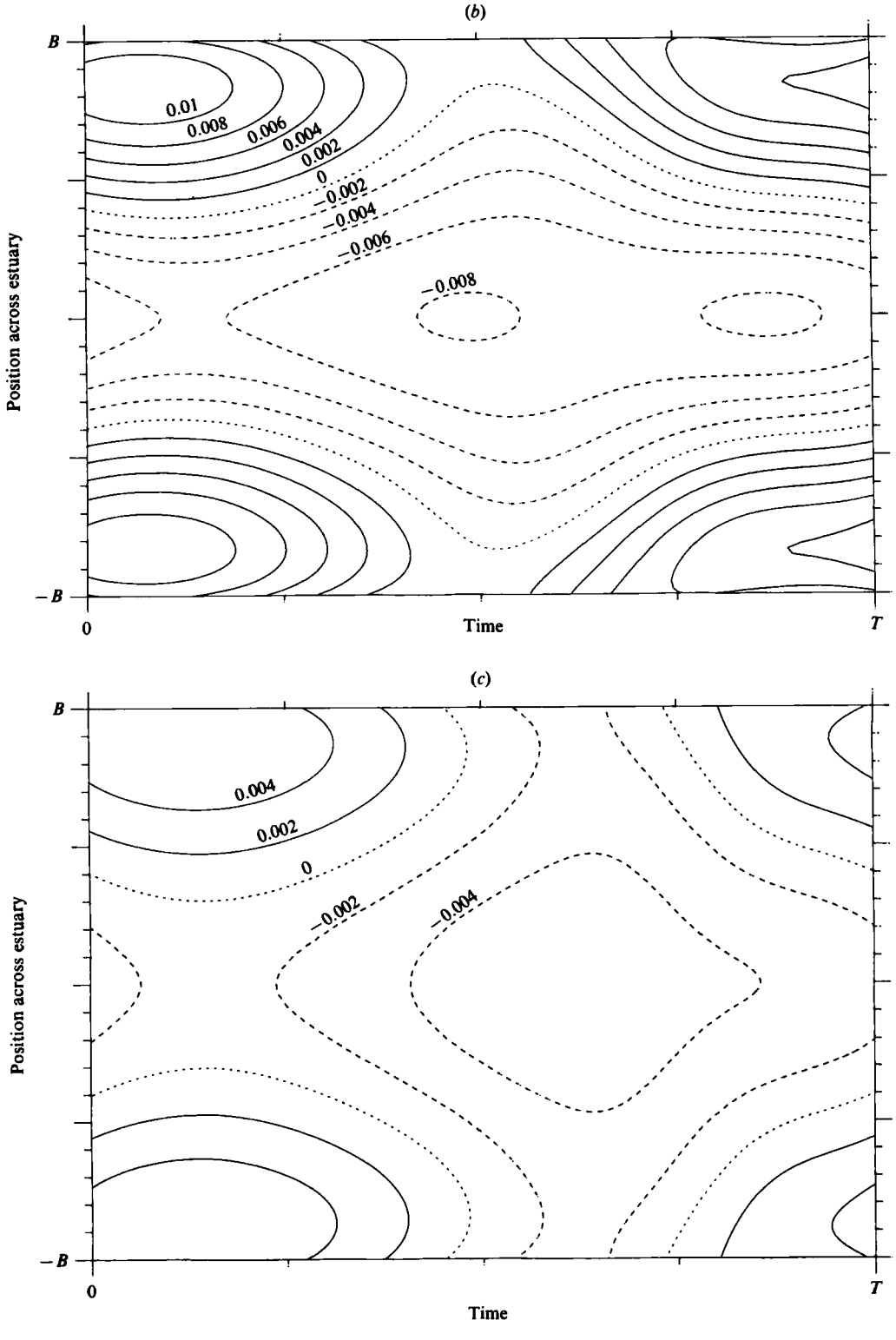

FIGURE 6(*b*) and (*c*). For description see opposite.

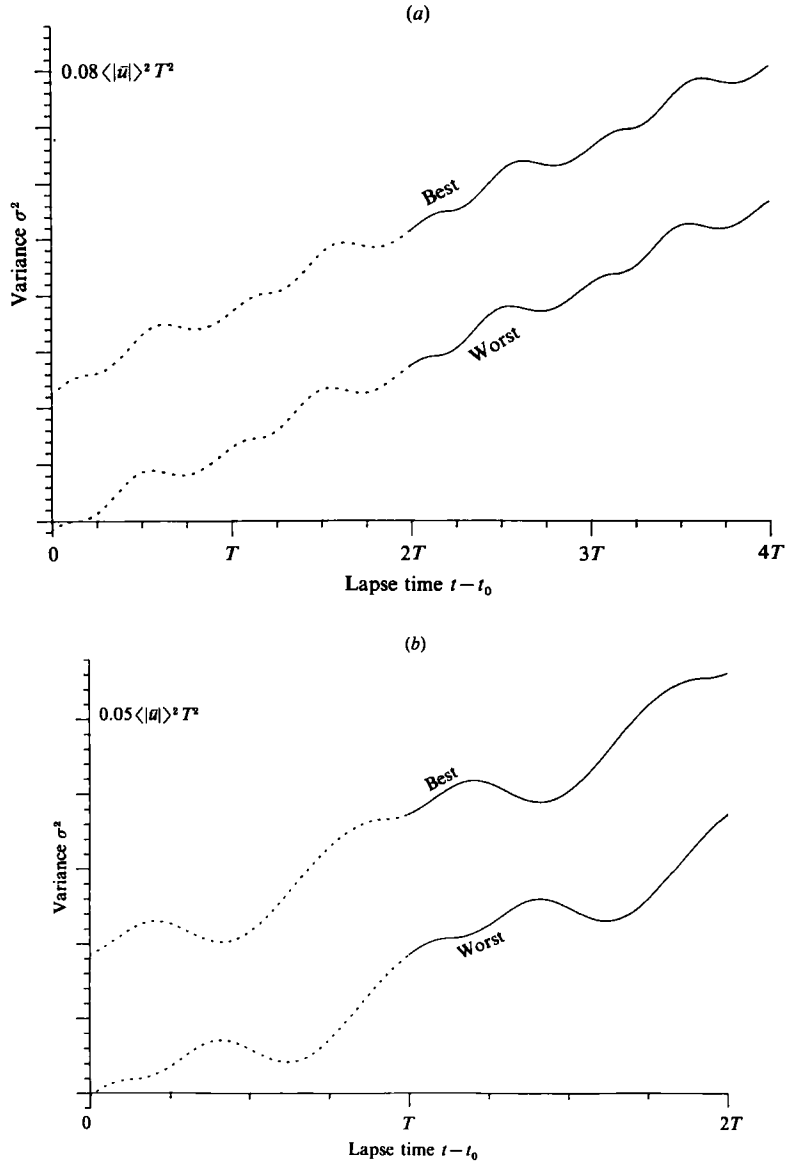

FIGURE 7 (*a*) and (*b*). For description see opposite.

The corresponding solution for the influence function $g_{-}^{(2)}$ simply involves the replacement of ξ by $1-\xi$.

For a point discharge we can split the formula (6.2) into symmetric source and observation terms. The source contribution to $\delta\sigma^2$ is

$$2\int_{t_0}^{t_*}[\overline{ug_-}-\langle D\rangle]\,\mathrm{d}t'+2g_{-}^{(2)}(y_0,z_0,t_0)-g_-(y_0,z_0,t_0)^2-\overline{g_-g_+}|_{t_*}, \tag{8.24}$$

where we have neglected the longitudinal turbulence contributions $\overline{\kappa}_{11}$ and K_-. To apply this formula we need to supplement the above results with the further result

$$\overline{g_+g_-}|_{t_*}=\frac{\langle|\bar{u}|\rangle^2T^2}{14\lambda^2}\left\{2-\tanh^2\tfrac{1}{2}\lambda-\frac{2\cosh\lambda(\xi_*-\frac{1}{2})}{\cosh\frac{1}{2}\lambda}\right\}. \tag{8.25}$$

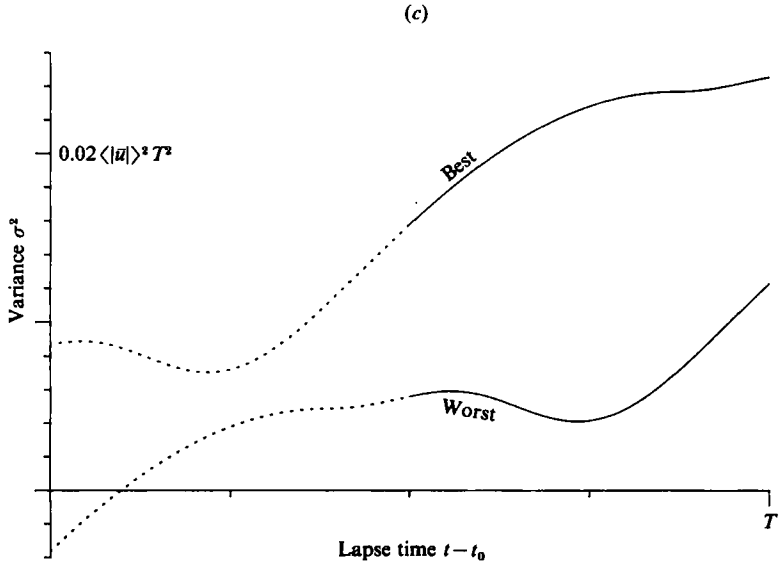

FIGURE 7. Variance at the side of the estuary as a function of the lapse time $\delta t = t - t_0$ for the best and worst discharge conditions. The non-dimensional mixing rates are (*a*) $\lambda = \frac{3}{2}$, (*b*) 3 and (*c*) 6. The asymptotic results are deemed to be unreliable in the dotted sections.

Figures 4 and 5 give numerical results for the optimal timing and position of point discharges in a sinusoidal flow. The dip in $\varkappa$ near flow reversal leads to a double-peaked behaviour for $\delta\sigma^2$ when λ is small. The discontinuity at $\lambda = 1.65$ in figures 4 and 5 corresponds to the changeover in dominance between the peaks either side of flow reversal.

To illustrate the behaviour of $\delta\sigma^2$, figures 6(*a–c*) give the source contribution (8.24) for sinusoidal flows with

$$t_* = 0, \quad \lambda = \tfrac{3}{2}, 3, 6. \tag{8.26}$$

As predicted in §7, there is a changeover from predominantly spatial to temporal behaviour as the mixing efficiency increases. There is also a marked reduction in the magnitude of the excess variance as λ increases.

The corresponding dependence of $\delta\sigma^2$ upon the observation conditions (y, z, t) can be obtained simply by replacing g_- and $g_-^{(2)}$ by g_+ and $g_+^{(2)}$ in (8.24). The symmetry with respect to time of the sinusoidal velocity field allows us to use the same figures 5 and 6(*a–c*) with the time axis reversed. The total excess variance $\delta\sigma^2$ is then the sum of the source and observation contributions.

To illustrate the magnitude of the source effect, figures 7(*a–c*) show the variance at the side of wide ($\lambda = \frac{3}{2}$), intermediate ($\lambda = 3$) and narrow ($\lambda = 6$) estuaries for the best and worst discharge conditions. The asymptotic formulae for σ^2 and $\delta\sigma^2$ are only valid after cross-sectional mixing has occurred. Thus the results are presented over time ranges of six times the e-folding time T_c, with the unreliable initial sections shown as dotted curves. In all three cases the timing and cross-stream position of the discharge has a substantial influence upon the spread, and hence upon the concentration, of the contaminant.

For other observation positions the results would be less oscillatory, and might not exhibit the contractions after flow reversal (Smith 1983). However, the division of

the excess variance $\delta\sigma^2$ into source and observation terms means that the separation between the best and worst curves would be unchanged. Indeed, for observations along the centreline of the estuary the total variance would be lower (see figures 6*a–c*), and the relative impact of the discharge conditions would be even more dramatic.

The financial support of the Royal Society is gratefully acknowledged.

Appendix. Upstream and downstream diffusion equations

In the above analysis we repeatedly require the evaluation of integrals of the form (see (2.3*b*))

$$\int_{t_0}^{t} \overline{(r-\bar{r})\,b}\,\mathrm{d}t', \tag{A 1}$$

where $b(y,z,t)$ satisfies a forced diffusion equation (see (2.4*a–c*))

$$\partial_t b - \boldsymbol{\nabla}\cdot(\boldsymbol{\varkappa}\cdot\boldsymbol{\nabla} b) = s-\bar{s}, \tag{A 2a}$$

with
$$\boldsymbol{n}\cdot\boldsymbol{\varkappa}\cdot\boldsymbol{\nabla} b = 0 \quad \text{on } \partial A, \tag{A 2b}$$

and
$$\bar{b} = 0. \tag{A 2c}$$

Hence b depends upon the value of s at earlier times. In the particular case $b = b^{(0)}$ the forcing is absent, i.e. $s = 0$.

From the weight factor $r(y,z,t)$ in the integral (A 1), we define an auxiliary function $a(y,z,t)$, which depends upon the value of r at later times:

$$-\partial_t a - \boldsymbol{\nabla}\cdot(\boldsymbol{\varkappa}\cdot\boldsymbol{\nabla} a) = r-\bar{r}, \tag{A 3a}$$

with
$$\boldsymbol{n}\cdot\boldsymbol{\varkappa}\cdot\boldsymbol{\nabla} a = 0 \quad \text{on } \partial A, \tag{A 3b}$$

and
$$\bar{a} = 0. \tag{A 3c}$$

If we multiply (A 2*a*) by $a(y,z,t)$, subtract (3*a*) multiplied by $b(y,z,t)$, and then integrate across the flow, we arrive at

$$\partial_t(\overline{ab}) = \overline{(s-\bar{s})\,a} - \overline{(r-\bar{r})\,b}. \tag{A 4}$$

Performing an integration with respect to time, we achieve our desired result

$$\int_{t_0}^{t} \overline{(r-\bar{r})\,b}\,\mathrm{d}t' = \overline{ab}|_{t_0} - \overline{ab}|_t + \int_{t_0}^{t} \overline{(s-\bar{s})\,a}\,\mathrm{d}t'. \tag{A 5}$$

From (A 2*a*) we see that $s(y,z,t)$ is two spatial derivatives simpler than the function $b(y,z,t)$. Indeed, in the particular case $b = b^{(0)}$ we have the ultimate simplification $s = 0$. In general, the component terms of s themselves satisfy a forced diffusion equation of the form (A 2*a*). Thus, after reorganization of the right-hand-side integrals to the form (A 1), the process can be repeated until finally an explicit formula is obtained.

The auxiliary function $a(y,z,t)$ represents the long-term influence of the discharge conditions. Hence it is appropriate that $a(y,z,t)$ should satisfy a time-reversed diffusion equation, and only depends upon what happens *after* the discharge takes place.

REFERENCES

ALLEN, C. M. 1982 Numerical simulation of contaminant dispersion in estuary flows. *Proc. R. Soc. Lond.* A **381**, 179–184.

ARIS, R. 1956 On the dispersion of a solute in a fluid flowing through a tube. *Proc. R. Soc. Lond.* A **235**, 67–77.

BOWDEN, K. F. 1965 Horizontal mixing in the sea due to a shearing current. *J. Fluid Mech.* **21**, 83–95.

CHATWIN, P. C. 1975 On the longitudinal dispersion of passive contaminant in oscillatory flows in tubes. *J. Fluid Mech.* **71**, 513–527.

DAISH, N. C. 1985 Optimal discharge profiles for sudden contaminant releases in steady, uniform open channel flow. *J. Fluid Mech.* (to appear).

FISCHER, H. B. 1972 Mass transport mechanisms in partially stratified estuaries. *J. Fluid Mech.* **53**, 671–687.

HOLLEY, E. R., HARLEMAN, D. R. F. & FISCHER. H. B. 1970 Dispersion in homogeneous estuary flow. *J. Hydraul. Div. ASCE* **96**, 703–724.

KREISS, H. 1957 Some remarks about nonlinear oscillations in tidal channels. *Tellus* **9**, 53–68.

SMITH, R. 1981 The importance of discharge siting upon contaminant dispersion in narrow rivers and estuaries. *J. Fluid Mech.* **108**, 45–53.

SMITH, R. 1982 Contaminant dispersion in oscillatory flows. *J. Fluid Mech.* **114**, 379–398.

SMITH, R. 1983 The contraction of contaminant distributions in reversing flows. *J. Fluid Mech.* **128**, 137–152.

SMITH, R. 1984 Temporal moments at large distances downstream of contaminant releases in rivers. *J. Fluid Mech.* **140**, 153–174.

YASUDA, H. 1982 Longitudinal dispersion due to the boundary layer in an oscillatory current: theoretical analysis in the case of an instantaneous line source. *J. Oceanogr. Soc. Japan* **38**, 385–394.